Journal of Alloys and Compounds 489 (2010) 336–338

Contents lists available at ScienceDirect

Journal of Alloys and Compounds

journal homepage: www.elsevier.com/locate/jallcom

Characterization of delafossite-type $CuCoO_2$ prepared by ion exchange

M. Beekman[a], J. Salvador[b], X. Shi[c], G.S. Nolas[a], J. Yang[b,*]

[a] Department of Physics, University of South Florida, Tampa, FL 33620, United States
[b] Materials and Processes Lab, General Motors Research and Development Center, Warren, MI 48090, United States
[c] Optimal Inc., Plymouth Township, MI 48170, United States

ARTICLE INFO

Article history:
Received 30 June 2009
Received in revised form
18 September 2009
Accepted 22 September 2009
Available online 30 September 2009

Keywords:
Delafossite
Oxide
Ion exchange synthesis
Metathesis reaction
Thermoelectric materials

ABSTRACT

Polycrystalline specimens of the delafossite oxide $CuCoO_2$ (space group $R\bar{3}m$, $a = 2.8494(2)$ Å, $c = 16.926(1)$ Å, $Z = 3$) were prepared by metathesis reaction between CuCl and $LiCoO_2$ at 590 °C and characterized by powder X-ray diffraction, thermal analysis, magnetic susceptibility, and electrical transport measurements. Decomposition of the title compound at 680 °C to its respective binary oxides was observed by thermal analysis. Electrical resistivity and magnetic susceptibility data for polycrystalline $CuCoO_2$ are consistent with formal charge assignments of Cu^+ and Co^{3+} for the transition metal constituents, while the room temperature Seebeck coefficient for the nominally undoped specimen was found to be −175 μV/K. The experimental data are consistent with recent density functional theory calculations for this material.

1. Introduction

The family of layered oxides generally referred to as delafossites derive their name from the mineral $CuFeO_2$ [1], with which their crystal structures are isotypic. Denoted by the general chemical formula ABO_2, the crystal structures of these materials (Fig. 1) are characterized by layers of distorted, edge-sharing octahedra with oxygen coordinating metal cations (B = typically transition or group 13 elements, but also some rare earth species), separated by planar layers of a transition metal (A = typically Cu, Ag, Pd, or Pt) which are linearly coordinated along the *c*-axis by two oxygen sites. The stacking orientation of these two layers results in two basic polymorphs, 2*H* (space group $P6_3/mmc$) and 3*R* (space group $R\bar{3}m$, Fig. 1).

Characterized by a wide range of possible compositions, the delafossite oxides also exhibit a significant richness in properties. For example, depending upon the choice of A, compounds can display metallic (A = Pd, Pt) or semiconducting/insulating (A = Cu, Ag) behavior [2]. Motivated by the relatively high electrical conductivities observed in some delafossite compounds [2–5], in particular observations [3,4] of p-type conductivity and relatively high optical transparency in $CuAlO_2$ thin films, significant efforts in recent years have focused on assessing the potential these materials hold in applications as transparent conductors [5].

Investigation of novel oxide materials for thermoelectric power generation applications is undertaken due to expected advantages in fabrication cost, materials stability, and environmental considerations, and is further motivated by reports of promising thermoelectric properties for several layered oxide compounds [6–8]. Very recently, it has been suggested [9–12] that some delafossite compounds, in particular the composition $CuCoO_2$ [10], might be of interest as candidate oxide materials for thermoelectric power generation. To date the $CuCoO_2$ delafossite has not been well characterized experimentally. $CuCoO_2$ has previously been prepared by hydrothermal [13] and solution-based [14] techniques, as well as thermal decomposition of copper–cobalt hydroxysalts [15]. Herein we used a straightforward solid-state ion exchange (metathesis) reaction [16] between CuCl and $LiCoO_2$ to prepare polycrystalline specimens of this delafossite composition. Thermal analysis, electrical transport, and magnetic susceptibility data for $CuCoO_2$ are presented.

2. Experimental details

CuCl (Alfa Aesar, 99.999%) and $LiCoO_2$ (Alfa Aesar, 99.5%) precursors were used for synthesis as received. All manipulations were carried out inside of an Ar-filled glove box, and additional precautions were taken to minimize exposure of the CuCl to light. Reactions were carried out in alumina crucibles, sealed inside evacuated silica tubes. Powder X-ray diffraction (p-XRD) data were collected with a Bruker D8 diffractometer in Bragg–Brentano geometry using Cu Kα radiation. Rietveld refinement was performed to determine lattice parameters using the GSAS [17] and EXPGUI [18] software. Thermal analysis data were collected with a TA Instru-

* Corresponding author at: Materials and Processes Lab, General Motors R&D Center, 30500 Mound Road, MC 480106224, Warren, MI 48090, United States.
Tel.: +1 586 986 9789; fax: +1 586 986 3091.
E-mail address: jihui.yang@gm.com (J. Yang).

0925-8388/$ – see front matter © 2009 Elsevier B.V. All rights reserved.
doi:10.1016/j.jallcom.2009.09.124

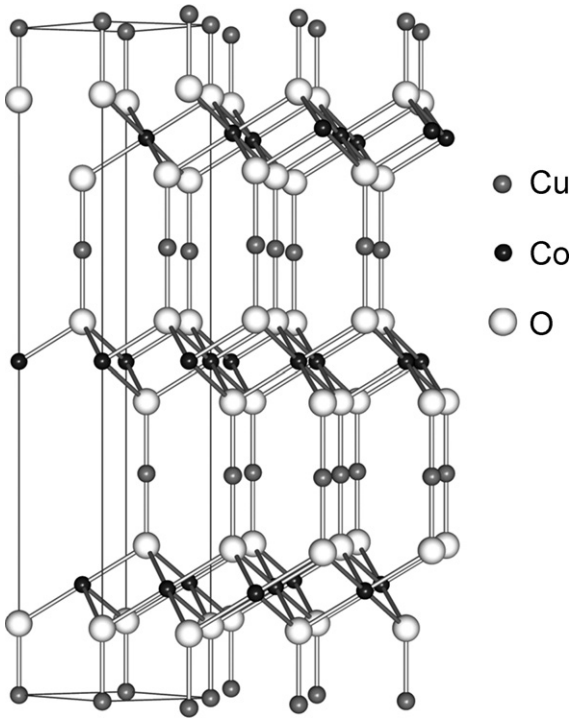

Fig. 1. A depiction of the $CuCoO_2$ 3*R*-delafossite crystal structure. The rhombohedral unit cell is outlined at left.

ments SDT Q600, using a heating rate of 20 °C/min under flowing N_2 gas in open alumina pans. Consolidation by spark plasma sintering (SPS) was conducted with a Sumitomo Dr. Sinter SPS system. Electrical resistivity (four-probe, low-frequency AC bridge technique) and magnetic susceptibility were measured using a Quantum Design MPMS. Room temperature Seebeck coefficient measurements were carried out by a steady-state method.

3. Results and discussion

Prior to establishing the effectiveness of the metathesis route, we note that initial attempts were also made to prepare the title compound by solid-state sintering reactions of the monoxides CuO and CoO in 1:1 ratios [19] under various conditions. These attempts resulted in multiphase mixtures containing $CuCo_2O_4$ [20] and/or binary oxides rather than the delafossite $CuCoO_2$. Metathesis routes have been successfully applied to the synthesis of several delafossite compositions [13,16,21,22]. As such, the ion exchange reaction:

$$CuCl + LiCoO_2 \rightarrow LiCl + CuCoO_2$$

was considered. This reaction was previously reported [16] to be successful for preparation of the $CuCoO_2$ composition. To facilitate diffusion, CuCl and $LiCoO_2$ were thoroughly ground together in the CuCl:$LiCoO_2$ ratio 1.03:1 (3 molar% excess CuCl to ensure complete reaction of $LiCoO_2$) with mortar and pestle in an argon-filled glovebox. The resulting mixture was cold pressed to form a pellet and then placed in an alumina crucible, then sealed in an evacuated silica ampoule for reaction in a furnace.

$CuCoO_2$ was successfully prepared reproducibly according to the above procedure by reaction at 590 °C for 2 days. The resulting products were washed thoroughly with distilled water to remove the LiCl product, which dissolves readily. Any remaining CuCl could be removed by brief washing with aqua regia. The resulting products were very fine, grayish powders consisting of $CuCoO_2$ as the major phase, with only small amounts of impurity phases. Fig. 2 shows calculated and experimental p-XRD patterns, confirming the $CuCoO_2$ 3*R*-delafossite crystal structure.

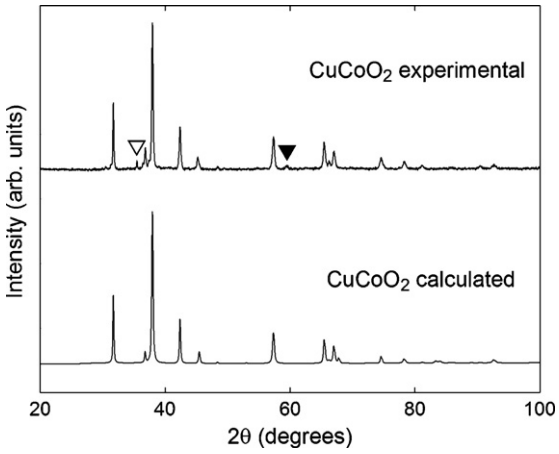

Fig. 2. Experimental (top) and calculated (bottom) powder X-ray diffraction patterns for a $CuCoO_2$ specimen synthesized at 590 °C. Weak reflections due to minor impurity phases of CuO (▽) and $LiCoO_2$ (▼) are indicated.

Weak reflections due to minor impurity phases CuO and $LiCoO_2$ are also indicated in Fig. 2. As shown, all other peaks are indexed to the $CuCoO_2$ phase, with the positions and relative intensities in good agreement. The unit cell parameters (space group $R\bar{3}m$) were determined from Rietveld refinement to be $a = 2.8494(2)$ Å and $c = 16.926(1)$ Å ($V = 119.016(2)$ Å^3). These values are in agreement with $a = 2.8488(1)$ Å and $c = 16.920(2)$ Å reported [13] for a $CuCoO_2$ specimen prepared by hydrothermal methods. We note strong absorption/fluorescence in our $CuCoO_2$ powdered specimen with Cu Kα radiation (due to Co) likely limits the detailed structural characterization from Rietveld refinement. Nevertheless, the p-XRD data clearly confirms the crystal structure of our $CuCoO_2$ specimen in agreement with previous results [13].

Differential thermal analysis (DTA) and thermogravimetric (TG) data for a $CuCoO_2$ specimen in the range of 200–1000 °C are shown in Fig. 3. No thermal events are observed until 680 °C, whereupon a prominent endothermic event commences. Two-step decomposition is thereafter observed, with an accompanying loss of weight presumably due to oxygen loss. p-XRD revealed the post-DTA/TG products consist of a mixture of the binary oxides CoO and Cu_2O, the latter metal-rich oxide being consistent with the observed weight loss.

The temperature dependent magnetic susceptibility, $\chi(T)$, for $CuCoO_2$ is shown in Fig. 4a. $\chi(T)$ remains negative in the entire temperature range with only a weak temperature dependence. We did not observe any ferromagnetic or paramagnetic impurity contribution from the specimen at temperatures as low as 2 K. These results contrast the magnetic susceptibility from $CuCoO_2$ described

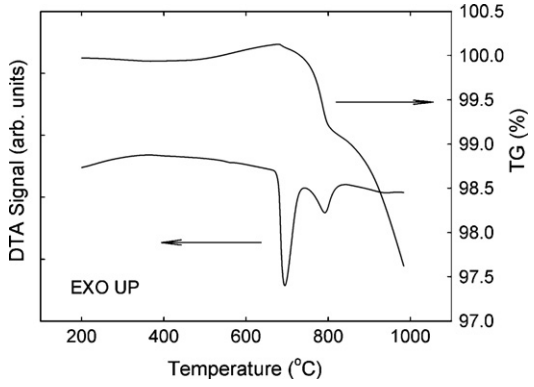

Fig. 3. DTA and TG curves for a $CuCoO_2$ specimen heated at 20 °C/min under flowing N_2.

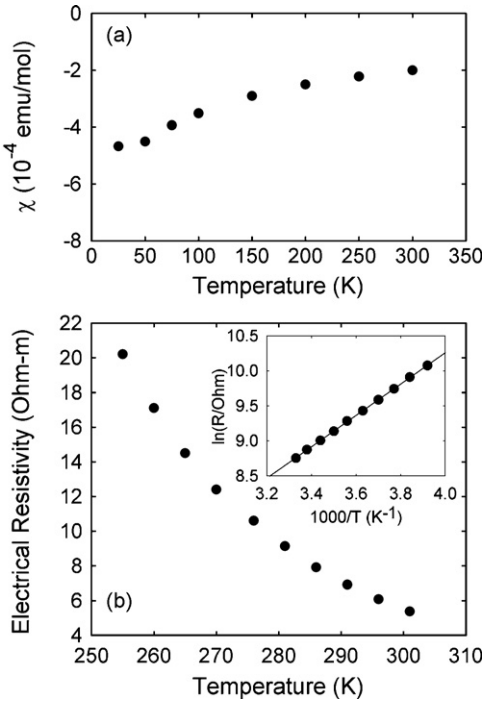

Fig. 4. (a) Magnetic susceptibility data for $CuCoO_2$, indicating diamagnetic response over the entire temperature range of measurement. (b) Electrical resistivity data for $CuCoO_2$ indicating an activated temperature dependence. Inset: Arrhenius plot, showing a fit to the data of the form $\rho(T) \sim \exp(E_a/k_BT)$.

in Ref. [16], in which a $CuCoO_2$ specimen was found to display paramagnetic susceptibility with a magnitude significantly higher than expected for this composition, indicating the presence of paramagnetic and/or ferromagnetic impurities [16]. The essentially temperature independent diamagnetism observed for our $CuCoO_2$ specimen is in better agreement with formal charge assignments of Cu^+ (d^{10}) and Co^{3+} (d^6, low spin) as suggested from the scheme given by Rogers et al. [2], as well as the analysis of the electronic band structure determined by density functional theory (DFT) calculations [10]. The data shown in Fig. 3 more likely reflect the intrinsic properties of the $CuCoO_2$ composition, and may indicate our specimen is closer to stoichiometry [16].

Consolidation of $CuCoO_2$ powders by SPS at 600 °C with an applied pressure of 45 MPa resulted in a compact that was 72% of the calculated density from XRD. At higher consolidation temperatures, partial or complete decomposition of the specimens was observed, consistent with the thermal analysis data discussed above. No significant preferential grain orientation was observed from p-XRD of the consolidated pellet. Electrical resistivity, $\rho(T)$, measurements were performed on a parallelepiped specimen cut from the SPS consolidated compact and are shown in Fig. 4b. The data show an activated temperature dependence, with $\rho(300\,K) \sim 5\,\Omega\,m$. An Arrhenius plot (inset to Fig. 4b) and corresponding fit indicate a temperature dependence of $\rho(T) \sim \exp(E_a/k_BT)$, where k_B is Boltzmann's constant and E_a is an activation energy for conduction. From the fit, we obtain $E_a = 0.2$ eV. The same value was previously reported [2] for conductivity measurements perpendicular to the *c*-axis on a small single crystal $CuCoO_2$ platelet. If the data in Fig. 4b represent intrinsic conduction (and assuming temperature independent carrier mobility), this would imply a band gap $E_g = 2E_a = 0.4$ eV, quite close to the value 0.38 eV predicted [10] from DFT calculations. Although the local density approximation used in the DFT calculations of Ref. [10] often underestimates electronic band gaps, it was noted that in the case of $CuCoO_2$ the LDA-predicted crystal field gap is expected to be representative of the true (experimental) value [10]. We note some prudence should be exercised in the interpretation of the data of Fig. 4b, since the relative density of the consolidated polycrystalline specimen is only 72%, and thus porosity and grain boundary contributions may affect the observed resistivity. We also note the data for this polycrystalline specimen should be interpreted as "averaged" transport over the distinct crystallographic directions in this anisotropic material. Measurement of the room temperature Seebeck coefficient yielded the value −175 μV/K for our nominally undoped specimen. This value for *S* can be compared to the value of approximately −100 μV/K (nearly the same for both in-plane and *c*-axis Seebeck coefficients) calculated for n-type doping of 0.02 carriers per formula unit using the DFT-calculated electronic structure and Boltzmann transport theory [10].

4. Conclusion

The delafossite oxide $CuCoO_2$ was successfully prepared in polycrystalline form *via* a relatively straightforward ion exchange (metathesis) solid-state reaction between CuCl and $LiCoO_2$. The title compound decomposed at 680 °C under flowing N_2 to corresponding binary oxides Cu_2O and CoO. Transport and magnetic susceptibility data for polycrystalline $CuCoO_2$ are consistent with formal charge assignments of Cu^+ and Co^{3+} for the transition metal constituents, and corroborate recent density functional theory calculations.

Acknowledgements

GSN and MB acknowledge support by the US Army Medical Research and Materiel Command under Award No. W81XWH-07-1-0708. M.B. also gratefully acknowledges support from the University of South Florida Presidential Doctoral Fellowship and a GM summer internship. JY, JRS, and XS thank Dr. Jan F. Herbst and Dr. Mark W. Verbrugge for continuous support and encouragement. The authors thank Dr. A. Datta for room temperature Seebeck measurements. This work was supported in part by GM and the U.S. DOE under corporate agreement DE-FC26-04NT42278.

References

[1] C. Friedel, C. R. Acad. Sci. (Paris) 77 (1873) 211.
[2] D.B. Rogers, R.D. Shannon, C.T. Prewitt, J.L. Gillson, Inorg. Chem. 10 (1971) 723.
[3] H. Kawazoe, M. Yasukawa, H. Hyodo, M. Kurita, H. Yanagi, H. Hosono, Nature 389 (1997) 939.
[4] H. Yanagi, S. Inoue, K. Ueda, H. Kawazoe, H. Hosono, J. Appl. Phys. 88 (2000) 4159.
[5] M.A. Marquardt, N.A. Ashmore, D.P. Cann, Thin Solid Films 496 (2006) 146.
[6] I. Terasaki, Y. Sasago, K. Uchinokura, Phys. Rev. B 56 (1997) R12685.
[7] R. Funahashi, I. Matsubara, H. Ikuta, T. Takeuchi, U. Mizutani, S. Sodeoka, Jpn. J. Appl. Phys. 39 (Pt. 2) (2000) L1127.
[8] K. Koumoto, I. Terasaki, R. Funahashi, Mater. Res. Soc. Bull. 31 (2006) 206.
[9] K. Isawa, et al., in: K. Koumoto (Ed.), Oxide Thermoelectrics, Research Signpost, Trivandrum, India, 2002, p. 213.
[10] D.J. Singh, Phys. Rev. B 76 (2007) 085110.
[11] D.J. Singh, Phys. Rev. B 77 (2008) 205126.
[12] S. Shibasaki, W. Kobayashi, I. Terasaki, Phys. Rev. B 74 (2006) 235110.
[13] R.D. Shannon, D.B. Rogers, C.T. Prewitt, Inorg. Chem. 10 (1971) 713.
[14] H.H. Emons, E. Beger, Z. Chem. 7 (1967) 200.
[15] P. Porta, R. Dragone, G. Fierro, M. Inversi, M.L. Jacono, G. Moretti, J. Chem. Soc. Faraday Trans. 88 (1992) 311.
[16] J.-P. Doumerc, A. Wichainchai, A. Ammar, M. Pouchard, P. Hagenmuller, Mater. Res. Bull. 21 (1986) 745.
[17] A.C. Larson, R.B. Von Dreele, General Structure Analysis System (GSAS), Los Alamos National Laboratory Report LAUR 86-748 (2004).
[18] B.H. Toby, J. Appl. Cryst. 34 (2001) 210.
[19] F. Bertaut, C. Delorme, C. R. Acad. Sci. 238 (1954) 1829.
[20] I. Rasines, J. Appl. Cryst. 5 (1972) 11.
[21] M. Shimode, M. Sasake, K. Mukaida, J. Solid State Chem. 151 (2000) 16.
[22] S. Park, D.A. Keszler, J. Solid State Chem. 173 (2003) 355.